182 variables (anisotropic thermal motion for non-hydrogen atoms, hydrogen atoms as fixed contributions, and an isotropic extinction parameter).

Acknowledgment. We thank the National Cancer Institute for their financial support of this research (Grant CA-12115).

Registry No. 1, 6675-72-5; **5**, 87556-04-5; **6**, 87585-15-7; **7**, 87556-05-6; **28**, 87556-06-7; **29**, 87556-07-8; **30**, 87556-08-9; **31**, 87556-09-0; **32**, 87556-10-3; **33**, 87678-00-0; **34**, 87556-11-4; **35**, 87556-12-5; **3l**, 87556-13-6; **3m**, 87556-14-7; **38**, 87585-16-8; **39**, 87556-15-8; **40**, 87556-16-9; **41**, 87585-17-9; **43**, 87556-17-0; **47**, 87556-18-1; **48**, 87556-19-2; **49**, 82950-40-1; **50**, 82918-62-5; **51**, 87556-20-5; **55a**, 87556-21-6; **55b**, 87556-22-7; **57**, 87556-23-8; **58**, 87556-24-9; **59**, 87585-18-0; **60**, 87585-19-1; **61**, 87556-25-0; chlorotrimethylsilane, 75-77-4; dimethyl acetylenedicarboxylate, 762-42-5; *N*-phenylmaleimide, 941-69-5; *N*-methyltriazolinedione, 13274-43-6; tetracyanoethylene, 670-54-2; maleic anhydride, 108-31-6; *N*-phenyltriazolinedione, 4233-33-4.

Supplementary Material Available: Figures 4 and 7 (unit cell stereodrawings of **43** and **47**) and final positional (Table V) and thermal (Table VI) parameters, observed and calculated structure factors (Table VII), bond lengths and angles (Table VIII), least-squares planes (Table IX), and torsional angles (Table X) for **43** and final positional (Table XI) and thermal (Table XII) parameters for non-hydrogen atoms, calculated positional and thermal parameters for hydrogen atoms (Table XIII), bond lengths and angles (Table XIV), least-squares planes (Table XV), torsional angles (Table XVI), and observed and calculated structure factors (Table XVII) for **47** (32 pages). Ordering information is given on any current masthead page.

Syntheses and ENDOR Investigations of ^{13}C-Labeled and Deuterated Phenalenyls. Rearrangement Reactions

Ch. Hass, B. Kirste, H. Kurreck,* and G. Schlömp

Contribution from the Institut für Organische Chemie der Freien Universität Berlin, 1000 Berlin 33, Germany. *Received March 8, 1983*

Abstract: Different synthetic routes to obtain ^{13}C-labeled, deuterated, and substituted phenalenyls are described. A rearrangement reaction has been discovered, probably of the Wagner–Meerwein type, that cannot be observed in the case of the unlabeled compound. ESR, ^{1}H, ^{2}H, ^{13}C, and ^{19}F ENDOR and TRIPLE experiments have been performed in fluid solution. Anisotropic hyperfine components have been obtained from liquid-crystal measurements. Relative signs of the hyperfine coupling constants have been determined by general TRIPLE resonance and by the interpretation of cross-relaxation effects observed in the ENDOR spectra. It is shown that the strong cross-relaxation effects of ^{13}C also significantly affect the relaxation properties of the protons.

Phenalenyl radical **1a** (perinaphthenyl) has proved to be very suitable in magnetic resonance investigations focusing on the properties of organic free radicals[1,2] or the development of new techniques.[3] This is due to its unique structure, being a planar hydrocarbon neutral radical of threefold symmetry, its stability, and its easy availability via several synthetic routes.[1,4-6] Moreover, phenalenyl is known to achieve high degrees of ordering in liquid-crystalline solutions (nematic and smectic phases).[5,7-10]

The present paper deals with ESR and ENDOR studies of ^{13}C-labeled phenalenyls. Studies of the isotropic and anisotropic ^{13}C hyperfine interactions provide a more detailed insight into the spin density distribution of a molecule than knowledge of the proton hyperfine interactions alone. In favorable cases it is possible to extract information on ^{13}C hyperfine splittings from the positions of natural abundance ^{13}C "satellite lines" observed in the ESR spectra. Actually, for phenalenyl this could be achieved in isotropic[2] as well as in liquid-crystalline solution.[5,7] However, this method usually fails with substituted phenalenyls because of the lowered symmetry decreasing the resolution of the ESR spectra. Attempts to observe ^{13}C ENDOR lines of phenalenyl in natural abundance have not been successful so far. This possibility is

Chart I

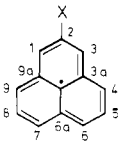

1 X = H
2 X = F
3 X = Cl

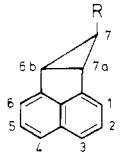

4 R = $COOC_2H_5$
5 R = COOH
6 R = COCl
7 R = $NH_3^+Cl^-$
8 R = Cl

a unlabelled
b ^{13}C-labelled, **1-3** -*-^{13}C, **4-8** -6b-^{13}C
c ^{13}C-labelled, **1-3** -2-^{13}C, **8** -7-^{13}C
bc ^{13}C-labelled, **3** -1,2-$^{13}C_2$,
d ^{2}H-labelled, **1** -2-H-d_8, **4-8** -7-H-d_8
e ^{2}H-labelled, **1** -1-H-d_8, **8** -6b-H-d_8

(1) P. B. Sogo, M. Nakazaki and M. Calvin, *J. Chem. Phys.*, **26**, 1343 (1957).
(2) F. Gerson, *Helv. Chim. Acta*, **49**, 1463 (1966).
(3) R. Biehl, M. Plato, and K. Möbius, *J. Chem. Phys.*, **63**, 3515 (1975).
(4) D. H. Reid, *Quart. Rev., Chem. Soc.*, **19**, 274 (1965).
(5) K. Möbius, H. Haustein, and M. Plato, *Z. Naturforsch., A*, **23a**, 1626 (1968).
(6) R. Biehl, Ch. Hass, H. Kurreck, W. Lubitz, and S. Oestreich, *Tetrahedron*, **34**, 419 (1978).
(7) S. H. Glarum and J. H. Marshall, *J. Chem. Phys.*, **44**, 2884 (1966). H. R. Falle and G. R. Luckhurst, *Mol. Phys.*, **11**, 299 (1966).
(8) K. P. Dinse, R. Biehl, K. Möbius, and H. Hausteln, *Chem. Phys. Lett.*, **12**, 399 (1971).
(9) R. Biehl, W. Lubitz, K. Möbius, and M. Plato, *J. Chem. Phys.*, **66**, 2074 (1977).
(10) (a) B. Kirste and H. Kurreck, *Appl. Spectrosc.* **34**, 305 (1980). (b) B. Kirste, *Chem. Phys. Lett.*, **83**, 465 (1981).

0002-7863/83/1505-7375$01.50/0

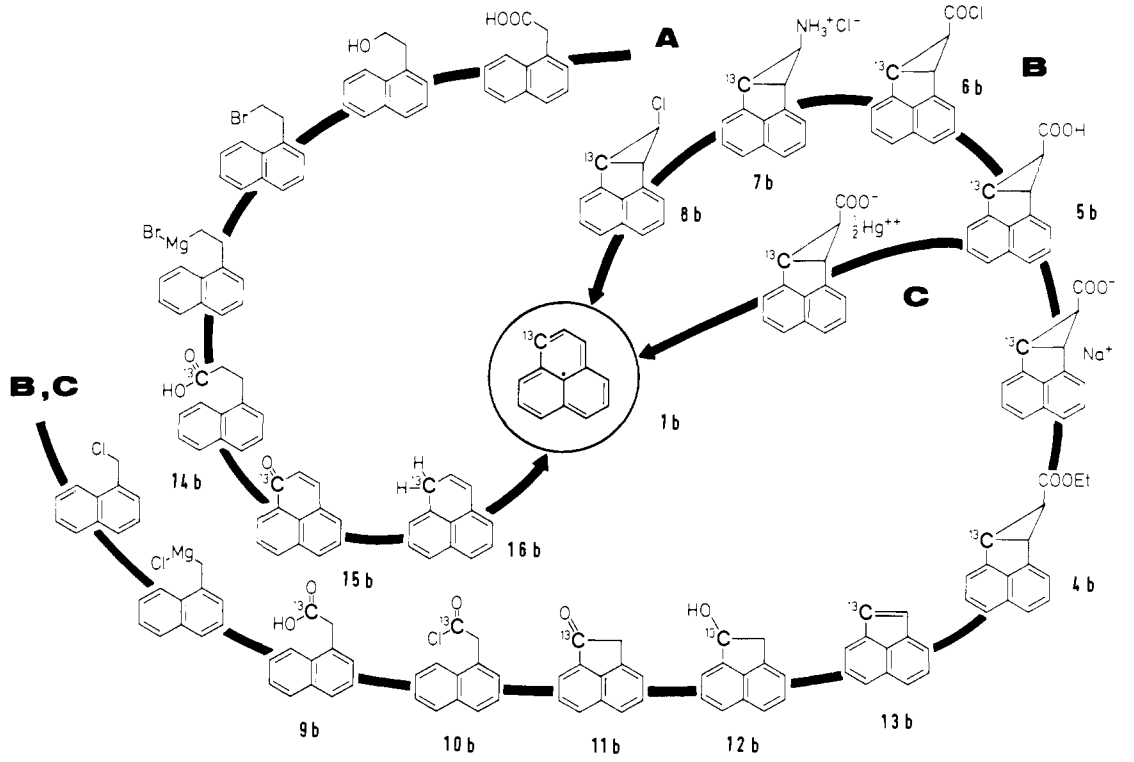

Figure 1. Reaction scheme and numbering of compounds.

apparently restricted to cases of exceptionally small ^{13}C hyperfine anisotropies.[11] Preparation of ^{13}C-enriched phenalenyls may allow measurements of ^{13}C hyperfine couplings by means of the more accurate ENDOR technique[12-14] and also (relative) sign determination by means of the general TRIPLE method.[3,15] Furthermore, it should be possible to study cross-relaxation effects,[13] which can also be used for the relative sign determination of hyperfine coupling constants.[16]

First, we report on several synthetic routes to ^{13}C-labeled phenalenyl and substituted phenalenyls. On an apparently unambiguous pathway[17,18] to phenalenyl-*1*-^{13}C (**1b**) via labeled 7-chloro-6b,7a-dihydro-7*H*-cycloprop[*a*]acenaphthylene (**8b**) we obtained substantial amounts of phenalenyl-*2*-^{13}C (**1c**) (Chart I). Further investigations showed that a rearrangement reaction occurs in the formation of **8b** which cannot be observed in the case of the unlabeled compound.

Syntheses. Phenalenyl radicals can be prepared as follows: (A) air oxidation of phenalenes,[4] (B) thermally induced cyclopropyl–allyl rearrangement with loss of a chlorine radical from 7-chloro-6b,7a-dihydro-7*H*-cycloprop[*a*]acenaphthylene (**8a**),[5,6] (C) thermal decarboxylation of the mercury salt of 6b,7a-dihydro-7*H*-cycloprop[*a*]acenaphthylene-7-carboxylic acid (**5a**),[6] and (D) reaction of acenaphthylene with halocarbenes (to give substituted phenalenyls).[6] These four methods can, in principle, be employed for the preparation of ^{13}C-labeled phenalenyls using commercial $Ba^{13}CO_3$ (^{13}C content 90% or 98%) as the starting material. Route A to phenalene-*1*-^{13}C (**1b**) proceeds via phenalenone-*1*-^{13}C (**15b**), and the introduction of $^{13}CO_2$ by Grignard reaction with (2-(1-naphthyl)ethyl)magnesium bromide, accessible from (1-naphthyl)acetic acid,[19] is straightforward (see Figure 1). Routes B–D are based on the reaction of acenaphthylene with carbenes, and the obvious starting materials for the synthesis of phenalenyl-*1*-^{13}C (**1b**) or -*2*-^{13}C (**1c**) are acenaphthylene-*1*-^{13}C (**13b**) or ^{13}C-labeled carbene precursors, respectively. Synthetic pathways B and C to **1b** are shown in the reaction scheme (Figure 1). Acenaphthylene-*1*-^{13}C (**13b**) is accessible from 1-(chloromethyl)naphthalene via Grignard reaction with $^{13}CO_2$ to **9b**, cyclization of the acid chloride **10b** to **11b** and reduction to **12b**, followed by dehydration. The preparation of **8b** then follows the reaction sequence described by Wittig et al.[20] and Pettit,[18] i.e., treatment of **13b** with ethyl diazoacetate yielding **4b**, followed by Curtius degradation to **7b** and substitution of the amino group by chloride after diazotization. However, whereas spectral evidence (^{13}C NMR, MS) proves that the reaction sequence takes the expected course until the formation of **7b**, the ^{13}C NMR spectra of "**8b**" reveal that the product obtained is actually a mixture containing about 15% of **8c** with the ^{13}C isotope in the "wrong" position 7 instead of 6b (vide infra). **1b** without admixture of **1c** could be prepared from **5b** via route C, i.e., by decomposition of the mercury salt, and via route A. ^{13}C-Labeled 2-chloro- and 2-fluorophenalenyls, **3b** and **2b**, have been obtained by a carbenoid synthesis (route D) from acenaphthylene-*1*-^{13}C (**13b**), using chloroform/potassium *tert*-butanolate[6] or sodium trifluoroacetate as carbene precursors, respectively. By use of $^{13}CHCl_3$, even the doubly labeled 2-chlorophenalenyl **3bc** could be prepared.

In view of the rearrangement observed in the formation of **8b**, we have reexamined the synthesis of the partially deuterated compounds **8d** and **1d**.[6] An H/D exchange with solvents could be avoided by using DCl in the hydrolysis of the isocyanate yielding the deuterated hydrochloride **7d**. It could be demonstrated that H/D exchange with solvents does not occur in the reaction **7d** → **8d** by treating the *unlabeled* hydrochloride **7a** with DCl/D_2O/AcOD: MS and ESR spectra proved the absence of deuterium in the products **8a** and **1a**. Nevertheless, the product "**8d**" was

(11) W. Lubitz, W. Broser, B. Kirste, H. Kurreck, and K. Schubert, *Z. Naturforsch., A*, **33a**, 1072 (1978). B. Kirste, W. Harrer, H. Kurreck, K. Schubert, H. Bauer, and W. Gierke, *J. Am. Chem. Soc.*, **103**, 6280 (1981).
(12) B. Kirste, H. Kurreck, W. Lubitz and K. Schubert, *J. Am. Chem. Soc.*, **100**, 2292 (1978).
(13) H.-J. Fey, W. Lubitz, H. Zimmermann, M. Plato, K. Möbius, and R. Biehl, *Z. Naturforsch., A*, **33a**, 514 (1978).
(14) For a general theory of nonproton ENDOR, see: M. Plato, W. Lubitz and K. Möbius, *J. Phys. Chem.*, **85**, 1202 (1981).
(15) K. Möbius and R. Biehl, "Multiple Electron Resonance Spectroscopy", M. M. Dorio and J. H. Freed, Eds., Plenum Press, New York, 1979, p 475.
(16) W. Lubitz and T. Nyrönen, *J. Magn. Reson.*, **41**, 17 (1980).
(17) R. Pettit, *Chem. Ind. (London)*, 1306 (1956).
(18) R. Pettit, *J. Am. Chem. Soc.*, **82**, 1972 (1960).
(19) J. Hoch, *Bull. Soc. Chim. Fr.*, **5**, 264 (1938). R. D. Haworth and C. R. Mavin, *J. Chem. Soc.*, **1933**, 1012. S. W. Pelletier and D. M. Locke, *J. Am. Chem. Soc.*, **79**, 4531 (1957).
(20) G. Wittig, V. Rautenstrauch, and F. Wingler, *Tetrahedron*, Suppl. 7, 189 (1966).

a mixture of **8d** and **8e**, containing about 30% of the latter.

Results and Discussion

Isotope Effects in IR Spectra. The IR spectra of the isotopically labeled compounds (^{13}C, ^{2}H) show shifts of most of the bands as compared with the unlabeled compounds, exclusively toward lower wavenumbers.[21] Although isotopic substitution has been used extensively in IR investigations of small molecules, only a few IR studies of ^{13}C- or ^{18}O-labeled complex organic molecules have been published.[22-24] The vibrational frequency ν of a diatomic oscillator is given by

$$\nu = (1/2\pi)(k/\mu)^{1/2} \quad (1)$$

where k is the force constant and μ the reduced mass, $\mu = m_1m_2/(m_1 + m_2)$. In an isotopically labeled compound, a different frequency ν^* is found because the reduced mass μ^* is changed:

$$\nu^*/\nu = (\mu/\mu^*)^{1/2} \quad (2)$$

Since the mode of the C=O stretching vibration is essentially localized, the calculated ratio for $^{13}C{=}O$ vs. $^{12}C{=}O$ is ν^*/ν = 0.9778. Experimentally we observed the following wavenumbers (cm^{-1}): **9b/9a**, 1655/1695; **10b/10a**, 1758/1796; and **11b/11a**, 1675/1715. These data agree within experimental error with the calculated shift of 38 cm^{-1}.[25]

NMR Spectra. Whereas mass spectroscopy is the method of choice for the determination of the overall contents of isotopic labels in a molecule, it is not normally useful in determining their positions unequivocally. Thus, the MS data showed ^{13}C contents of 90.7% in "**8b**" (starting material: $Ba^{13}CO_3$, 90% ^{13}C), and the degree of deuteration in "**8d**" was found to be 99.6% (97.1% D_8), excluding any intermolecular exchange. ^{13}C NMR was employed for the determination of the ratio of ^{13}C enrichment at the three-membered ring positions in compounds **7b** and **8b**. In order to obtain the correct intensities, the "inverse gated decoupling" method of the $^{13}C\{^1H\}$ double-resonance technique was employed.[26]

The ^{13}C NMR spectrum (67.89 MHz) of **7b** shows only one intense peak (δ_{TMS} 44.8); all other peaks are of low intensity, obviously due to ^{13}C in natural abundance. Apparently, the ^{13}C label in **7b** is located exclusively (within experimental error, >97%) in position 6b as expected. The spectrum of **8b**, however, shows two intense peaks with an intensity ratio of 84.5:15.5 (δ_{TMS} = 34.5 and 45.1), assigned to positions 6b and 7, respectively. Consequently, compound "**8b**" is actually a mixture of **8b** and the rearranged product **8c**.

^1H NMR spectra (270 MHz, $CDCl_3$) were taken from **8a** and the deuterated compound **8d**. The aliphatic protons in **8a** give rise to a doublet (δ 3.28, J = 1.9 Hz, positions 6b and 7a) and a triplet (δ 2.79, position 7). The spectrum of **8d** shows two sharp singlets at δ 2.78 and 3.27 with an intensity ratio of 69.0:31.0. Since no coupling is observed, these protons cannot be present within the same molecule. Thus, we must conclude that compound "**8d**" consists of a mixture of the two species **8d** (69%, proton in position 7) and **8e** (31%, proton in position 6b or 7a), vide infra. The remaining aromatic protons in **8d**, due to incomplete deuteration, give rise to singlets at δ 7.33, 7.35, and 7.52. The total intensity of the peaks in the aromatic region only amounts to about 3% of the absorption due to the proton in the three-membered ring. This result is consistent with the degree of deuteration determined by MS.

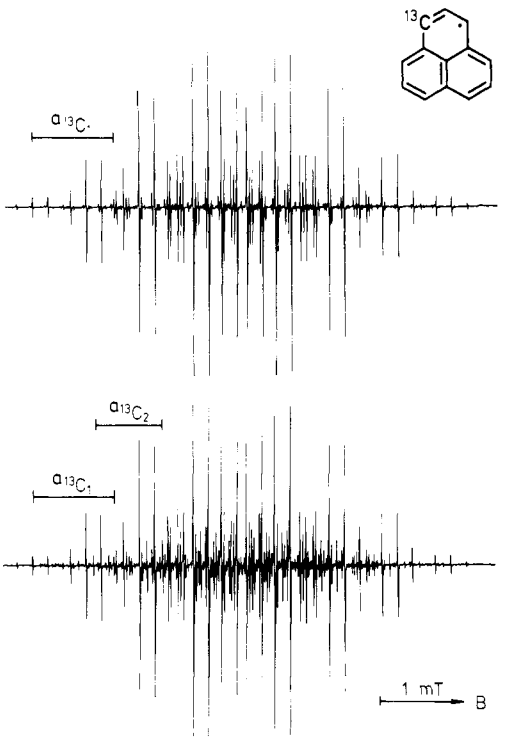

Figure 2. ESR spectra of phenalenyl-*1*-^{13}C (**1b**; toluene, room temperature) obtained via different pathways: top, radical obtained from the mercury salt of **5b** (route C); bottom, radical obtained from **8b** (route B). Note that additional ESR lines due to phenalenyl-*2*-^{13}C (**1c**) show up in the bottom spectrum (see text); the spectrum of unlabeled phenalenyl (**1a**, 10%) is superimposed to both spectra.

ESR Measurements in Isotropic Solution. Figure 2 shows the ESR spectra of ^{13}C-labeled phenalenyl obtained via two synthetic pathways supposed to produce phenalenyl-*1*-^{13}C (**1b**, 90% enrichment). The upper spectrum, from a sample generated by decomposition of the mercury carboxylate (route C), is easily interpreted to be a superposition of the spectra of phenalenyl-*1*-^{13}C and unlabeled phenalenyl. With the assumption of equal line widths, which is obviously a reasonable approximation for the conditions under consideration (toluene, room temperature), a ratio of 90:10 is obtained from the ESR amplitudes of the two species in accordance with the isotopic contents of the precursor.

Essentially the same spectrum was observed from a sample generated by air oxidation of the phenalene **16b** (route A; with a ratio of 96:4 for the two species reflecting the higher ^{13}C contents of the precursor). However, in the lower spectrum, from a sample generated by thermolysis of **8b** (route B), additional lines show up. From a comparison of the positions of these lines with those of the ^{13}C satellites in unlabeled phenalenyl and the total width of the respective spectrum a tentative assignment to phenalenyl-*2*-^{13}C (or phenalenyl-*3a*-^{13}C) is possible (vide infra, ENDOR results). Judging from the ESR amplitudes, the mixture consists of phenalenyl-*1*-^{13}C, phenalenyl-*2*-^{13}C, and unlabeled phenalenyl in the ratio 75:15:10, which is consistent with the isotopic distribution in the precursor **8b** as determined by NMR. It should be noted that the ESR lines of phenalenyl-*1*-^{13}C are severely broadened in highly viscous solvents, whereas those of unlabeled phenalenyl within the same sample remain comparatively narrow (e.g., 45 μT vs. 14 μT; mineral oil, Shell Ondina G33, room temperature). This behavior can be explained by the large ^{13}C hyperfine anisotropy (vide infra).

The ESR results for the ^{13}C-labeled phenalenyls demonstrate that no further rearrangement occurs in the final step of the synthesis (**8b** → **1b**) except for the cyclopropyl–allyl conversion, which does not affect the isotopic distribution. This statement also holds for the deuterated phenalenyls. Thus, thermolysis of "**8d**" yields a mixture of **1d** and **1e** with the remaining proton in position 2 or 1, respectively. A computer-simulated spectrum assuming a ratio of 69:31 for **1d/1e** (cf. NMR results for **8d**) shows

(21) H. Siebert, "Anwendungen der Schwingungsspektroskopie in der anorganischen Chemie", Springer-Verlag, Berlin, 1966.
(22) G. J. Karabatsos, *J. Org. Chem.*, **25**, 315 (1960).
(23) B. H. Baxter and A. F. C. Horsler, *Nature (London)*, **204**, 675 (1964). S. Brodersen, J. Christoffersen, B. Bak, and J. T. Nielsen, *Spectrochim. Acta*, **21**, 2077 (1965). P. Egli, *Appl. Spectrosc.*, **30**, 467 (1976). P. C. Painter and J. L. Koenig, *Spectrochim. Acta, Part A*, **1977A**, 1003.
(24) M. Halmann and S. Pinchas, *J. Chem. Soc.*, 1703 (1958).
(25) For further details, see: Ch. Hass, Thesis, FU Berlin, 1982.
(26) E. Breitmaier and G. Bauer, "^{13}C-NMR-Spektroskopie", Georg-Thieme-Verlag, Stuttgart, 1977.

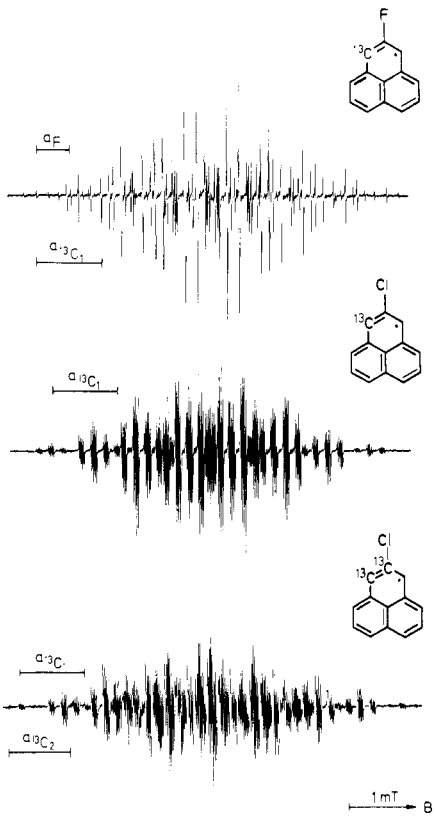

Figure 3. ESR spectra of **2b** (top), **3b** (center), and **3bc** (bottom) taken in toluene at room temperature.

good agreement with the experimental spectrum. An ESR spectrum of radical **1d** without rearrangement products could be obtained from a sample prepared via route C.[6]

The fully resolved ESR spectrum of 2-fluorophenalenyl (**2a**) consists of 42 lines due to hyperfine interactions with sets of two and six protons and the fluorine nucleus ($|a_F|$ = 14.3 MHz). Introduction of a ^{13}C nucleus gives rise to another splitting and thus a doubling of the number of hyperfine components; the spectrum of **2b** is depicted in Figure 3 (top). The ESR spectrum of 2-chlorophenalenyl (**3a**), previously published,[6] consists of seven triplets, each component being split into quartets due to the ^{35}Cl/^{37}Cl hyperfine interaction ($I = {}^3/_2$). Figure 3 shows the ESR spectra of the ^{13}C-labeled radical **3b** (center) and the doubly labeled **3bc** (bottom).

ENDOR. ENDOR spectra of phenalenyl-*1*-^{13}*C* (**1b**) dissolved in toluene could be recorded in the temperature range from about 260 to 320 K with a fairly good signal-to-noise ratio. (Because of a dimerization reaction, the radical concentration was insufficient at lower temperatures.) Spectra obtained for different field settings are shown in Figure 4. For comparison, the spectrum of unlabeled phenalenyl (**1a**) obtained by saturating a respective ESR component in the same sample is also included in Figure 4 (bottom). According to the ENDOR resonance condition

$$\nu_{ENDOR} = |\nu_n \pm a_n/2| \qquad (3)$$

it shows two pairs of ^{1}H ENDOR lines equally spaced about the free proton frequency (ν_H = 14.62 MHz). The poorer signal-to-noise ratio of this spectrum reflects the lower concentration (~10%) of the unlabeled species. In the ENDOR spectra of the ^{13}C-labeled radical, an additional line shows up at 9.80 MHz which can be identified as the low-frequency ^{13}C ENDOR line. Accidentally the high-frequency ^{13}C ENDOR line coincides with one of the ^{1}H ENDOR lines (17.16 MHz). Since $|a_1^C/2| > \nu_C$, the ^{13}C ENDOR lines appear equally spaced about $a_1^C/2$ = 13.48 MHz, separated by $2\nu_C$ = 7.36 MHz. The hyperfine coupling constants are collected in Table I. A striking feature of the spectra is the markedly different intensity pattern obtained when either a high- or a low-field ESR component is saturated. (It should be noted that the radio-frequency power is not constant over the whole frequency range but varies in a somewhat irregular fashion due to our experimental arrangement. Yet the experimental conditions were the same for both field settings.) The low-frequency ^{13}C ENDOR line is much more intense when a high-field ESR component (i.e., $a_1^C M_I^C < 0$) is saturated as compared to the low-field setting ($a_1^C M_I^C > 0$). Such behavior is usually found for nuclei exhibiting a large hyperfine anisotropy and is caused

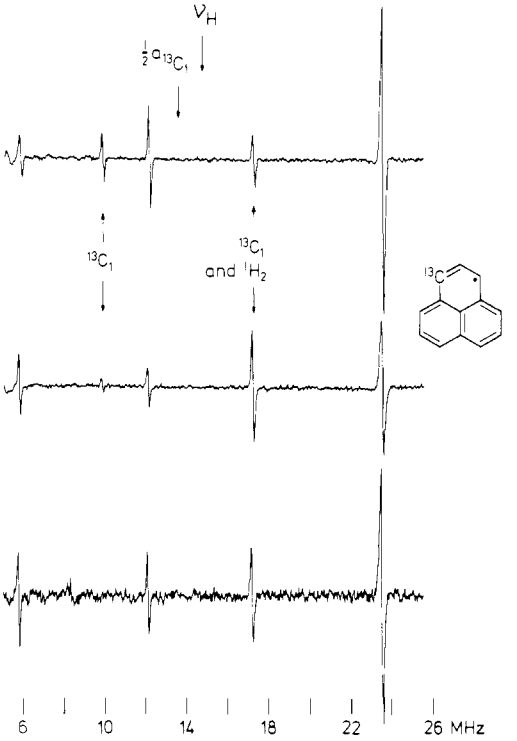

Figure 4. ENDOR spectra of **1b** (toluene, 290 K) obtained when saturating different ESR components: top, high-field setting; center, low-field setting; bottom, ENDOR spectrum of unlabeled phenalenyl (**1a**) taken by saturating a respective ESR component in the same sample (cf. Figure 2).

Table I. Isotropic Hyperfine Coupling Constants (MHz)[a]

position	1b,c	2b	3bc
1,3,4,6,7,9	−17.67	−17.64[b]	−17.70
(2),5,8	+5.09	+5.08	+5.08
2-^{19}F; $^{35/37}$Cl		−14.30	10.68[c]
1-^{13}C	+26.96	+26.76	+27.28
2-^{13}C	−21.90		−25.98

[a] Measured by ENDOR, solvent toluene, 290 K; accurate within ±0.02 MHz. Relative signs from TRIPLE measurements. [b] Inequivalence resolved in mineral oil (Shell Ondina G17, 290 K), −17.72 MHz (4 H), −17.50 MHz (2 H). [c] Measured by ESR.

Table II. Intensity Ratios, *R*, of the High-Frequency ENDOR Lines[a]

position	1b	1c	2a	2b[c]	3b
1-^{1}H	0.4	1.3	1.4	0.7	0.4
2-^{1}H	2.5[b]	0.9	0.6	1.4	1.7
1-^{13}C	3[b]			1.9[b]	4
2-^{13}C		1.5			
^{19}F			2.4	0.6	

[a] Calculated according to $R = E_{lf}/E_{hf}$, where E_{lf} and E_{hf} denote the amplitudes of the high-frequency ENDOR lines obtained with a field setting on the most intense low- or high-field ESR component, respectively. [b] Determined from the amplitudes of the low-frequency ENDOR lines ($R = E_{hf}/E_{lf}$). [c] Note that the selected (most intense) ESR components are superpositions of two hyperfine components. The dominant components are due to nuclear spin configurations $M_I^C = +{}^1/_2$, $M_I^F = +{}^1/_2$ (low-field) or $M_I^C = -{}^1/_2$, $M_I^F = -{}^1/_2$ (high-field), yet the opposite configurations give a contribution of 27%.

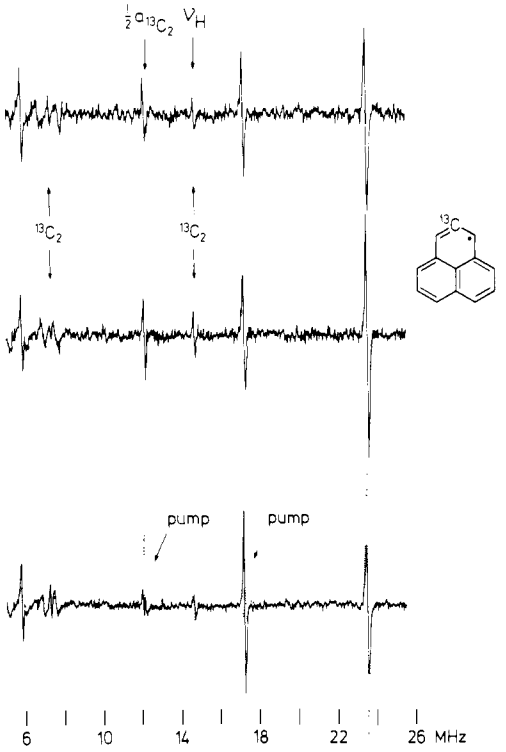

Figure 5. ENDOR spectra of **1c** (toluene, 290 K) obtained when saturating ESR components assigned to this radical (cf. Figure 2, bottom): top, high-field setting; center, low-field setting; bottom, general TRIPLE spectra of **1c**. The arrows indicate the setting of the pump frequency in the respective experiment.

by cross-relaxation effects $W_{x2}^{C} > W_{x1}^{C}$.[13,27] Moreover, this cross-relaxation effect due to the ^{13}C nucleus also manifests itself in the amplitude ratios of the ^{1}H ENDOR lines; *it cannot be observed in unlabeled phenalenyl.* The amplitude ratios are collected in Table II and will be discussed below.

It is noteworthy that relatively strong ^{13}C ENDOR lines could be observed in toluene at low rf power levels ($B_{NMR} \sim 0.4$ mT in the rotating frame) with line widths comparable to those of the protons (about 60 kHz). The relative intensity of the ^{13}C ENDOR lines increases only by about 20% when the temperature is increased from 260 to 320 K (toluene). In contrast, if a solvent of much higher viscosity is used, e.g., mineral oil at room temperature, only proton lines show up in the ENDOR spectrum of **1b**.

As was mentioned above, the ESR spectrum obtained from a sample generated by thermolysis of **8b** indicates the presence of a third species identified as phenalenyl-*2*-^{13}C (**1c**). ENDOR spectra could be recorded also from this species by saturating the respective ESR components (see Figure 5). They show two non-proton ENDOR lines besides ^{1}H ENDOR lines characteristic of phenalenyl. Since the separation between these lines amounts to 7.38 MHz = $2\nu_C$, they obviously have to be assigned to a ^{13}C coupling, $|a_2^{C}|$ = 21.90 MHz. It should be pointed out that the ENDOR experiment, in contrast to ESR, yields information about the kind of nucleus giving rise to a hyperfine splitting. Thus, the assignment to phenalenyl-*2*-^{13}C (**1c**) is confirmed. Cross-relaxation effects do also show up in the ENDOR spectra of **1c**, yet they are less pronounced than in the case of **1b** (see Table II).

Relative sign determination of all hyperfine couplings in **1b** and **1c** could be achieved by general TRIPLE experiments (see Figure 5, bottom). The absolute signs given in Table I are based on the assumption that large spin populations are positive (position 1 in phenalenyl); hence $a_1^{H} < 0$. Opposite signs were deduced for the two ^{13}C couplings in agreement with previous sign determinations from liquid-crystal studies of ^{13}C hyperfine shifts (natural abundance).[5,7]

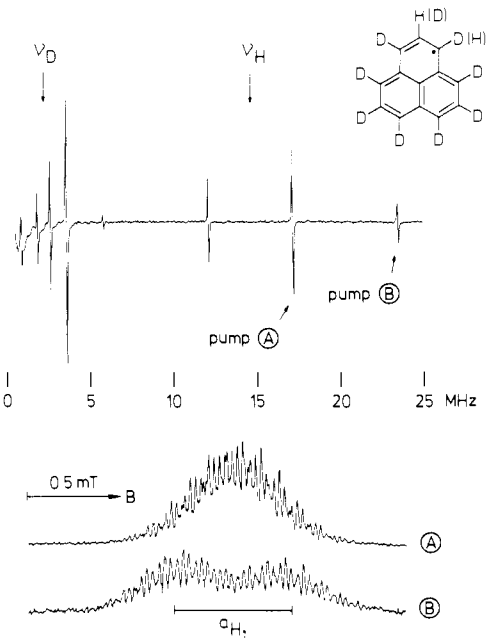

Figure 6. Top, ENDOR spectrum spectrum of "**1d**" (obtained from "**8d**"; mineral oil, Shell G17, 290 K); bottom, ENDOR-induced ESR spectra obtained when monitoring ENDOR peaks labeled A or B, respectively. Note that spectrum B is actually due to **1e** (see text).

The ENDOR spectrum of phenalenyl-d_8 (**1d**, from **8d**) shows two pairs of ^{2}H ENDOR lines centered about ν_D and two pairs of ^{1}H ENDOR lines centered about ν_H (see Figure 6, top). The deuterium couplings are smaller than the respective proton couplings by about the ratio of the magnetogyric ratios γ_D/γ_H. Since the appearance of ^{1}H ENDOR lines belonging to the large splitting a_1^{H} is not consistent with the structure **1d**, ENDOR-induced ESR experiments were performed.[28] The ENDOR-induced ESR spectra obtained with rf settings on the high-frequency line of either the small (A) or the large (B) proton splitting (see Figure 6) are quite different, proving that different species are involved. They can be identified as **1d** and **1e**, confirming the ESR results (vide supra).

In the ENDOR spectra of 2-fluorophenalenyl (**2a**; toluene, 290 K) two ^{19}F ENDOR lines show up symmetrically placed about the free ^{19}F frequency (ν_F = 13.79 MHz) in addition to two pairs of ^{1}H ENDOR lines centered about the free proton frequency (ν_H = 14.65 MHz). The relative line intensities are strongly influenced by cross-relaxation effects (see Table II). If mineral oil is used as solvent, ^{19}F ENDOR lines cannot be seen at 290 K owing to the higher viscosity of the solvent. Yet the ^{1}H ENDOR line widths are smaller thus allowing the resolution of a slight inequivalence of the large proton splittings. If the temperature is raised, ^{19}F ENDOR lines appear in the spectrum (above 330 K). A general TRIPLE experiment yielded a negative sign for the ^{19}F hyperfine coupling.

ENDOR spectra could also be recorded from 2-fluorophenalenyl-*1*-^{13}C (**2b**; toluene, 290 K) (see Figure 7). They show ^{1}H, ^{13}C, and ^{19}F ENDOR lines centered about ν_H, $a_1^{C}/2$, and ν_F, respectively. As in the case of **1b**, the high-frequency ^{13}C ENDOR line coincides with one of the ^{1}H ENDOR lines ($\sim$17.15 MHz) within the ENDOR line width. Again, the intensity pattern is affected by cross-relaxation effects (vide infra) (see Table II).

The ENDOR spectra of 2-chlorophenalenyl-*1*-^{13}C (**3b**) and the doubly labeled 2-chlorophenalenyl-*1*,*2*-$^{13}C_2$ (**3bc**) taken in toluene at 290 K are depicted in Figure 8. They show two pairs of ^{1}H ENDOR lines and one or two pairs of ^{13}C ENDOR lines, respectively. Interestingly the high-frequency ^{13}C ENDOR line from

(27) (a) D. S. Leniart, J. C. Vedrine, and J. S. Hyde, *Chem. Phys. Lett.*, **6**, 637 (1970). (b) W. Lubitz, K. P. Dinse, K. Möbius, and R. Biehl, *Chem. Phys.*, **8**, 371 (1975).

(28) J. S. Hyde, *J. Chem. Phys.*, **43**, 1806 (1965). N. M. Atherton and A. J. Blackhurst, *J. Chem. Soc., Faraday Trans. 2*, **68**, 470 (1972).

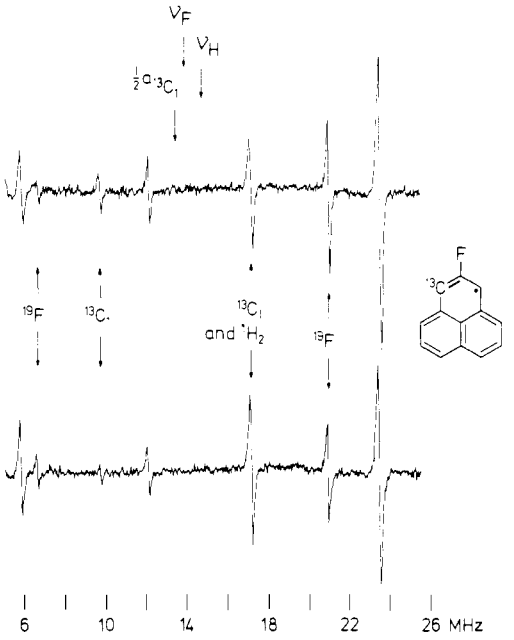

Figure 7. ENDOR spectra of **2b** (toluene, 290 K) obtained with the field set on the most intense high- (top) or low-field (bottom) ESR component (see Figure 3, top, and footnote *c* of Table II).

Figure 8. ENDOR spectra of **3b** (toluene, 290 K) obtained when the most intense high- (top) or low-field (center) ESR component is saturated (see Figure 3, center). Bottom, ENDOR spectrum of **3bc** (toluene, 290 K, center-field setting).

^{13}C in position 1 could be resolved in this case since the ^{13}C coupling constant is slightly larger than in the unsubstituted compound (see Table I). A much stronger increase in magnitude is found for the coupling constant of ^{13}C in position 2.[29] $^{35}Cl/^{37}Cl$ ENDOR lines could not be obtained as expected on account of the small isotropic coupling constant (0.68 MHz), the inconveniently low-lying free chlorine frequency ($\nu_{^{35}Cl}$ = 1.44 MHz) and the large quadrupolar interaction.[14]

(29) B. Kirste, H. Kurreck, H.-J. Fey, Ch. Hass, and G. Schlömp, *J. Am. Chem. Soc.*, **101**, 7457 (1979).

Table III. Anisotropic Hyperfine Shifts Measured in Nematic Phases (MHz)[a]

position	1b,c[b]	2a[c]	3b[b]
1,3,4,9	+0.04	−0.21, −0.18	−0.73
6,7	+0.04	+0.58	+1.63
(2),5,8	+0.63	+0.69	+0.73
2-^{19}F; $^{35/37}Cl$		+8.4	10.5[d]
1-^{13}C	−11.0		−11.6
2-^{13}C	+3.13		(+3.6)[e]

[a] Proton data from ENDOR measurements, nonproton data from ESR. [b] Solvent, nematic phase IV, 294 K. [c] Solvent, 4-cyano-4'-pentylbiphenyl, 294 K. [d] The Cl hyperfine splitting is not resolvable in the nematic phase. Shift and isotropic coupling have opposite signs. [e] Extrapolated value (3c), from ref 29.

Liquid-Crystal Measurements. In order to obtain information about the anisotropic hyperfine interactions and thus about the π spin populations, measurements in nematic mesophases were performed. Owing to the high viscosity of these phases, ^{13}C and ^{19}F ENDOR signals could not be observed, and the respective hyperfine splittings had to be taken from the ESR spectra. On passing from the isotropic to the nematic phase, the partial alignment of the dissolved radicals causes a shift in the observed hyperfine splittings due to contributions from the anisotropic hyperfine interaction:[30]

$$\Delta a = O_{33}A'_{33} + \tfrac{1}{3}(O_{11} - O_{22})(A'_{11} - A'_{22}) \quad (4)$$

where O_{ii} and A'_{ii} are the elements of the traceless ordering and hyperfine tensors, respectively. Provided that either the ordering or the hyperfine tensor is axially symmetric, the second term in eq 4 is zero:

$$\Delta a = O_{33}A'_{33} \quad (5)$$

The measured anisotropic hyperfine shifts are collected in Table III. With the experimentally determined hyperfine tensor data from ref 10b, the ordering parameter $O_{33} = -0.30 \pm 0.01$ is obtained for phenalenyl in phase IV at 294 K. A detailed analysis of the hyperfine shifts of 2-chlorophenalenyl (**3a**) has been given in a previous paper.[29] An important finding was that the ordering tensor deviates considerably from axial symmetry ($O_{33} = -0.30$, $O_{11} - O_{22} = +0.29$, phase IV, 294 K); i.e., the radicals are aligned preferentially with the C–Cl bond axis parallel to the director. As a consequence, substantially different shifts are measured for the protons at the positions 1, 3, 4, 9, and 6, 7 (see Table III). The results now obtained for **2a** show that the fluoro substituent also causes an additional alignment of the molecules, yet to a smaller extent than the larger chloro substituent. An analysis based on anisotropic hyperfine tensors given in ref 29 yields the following order parameters: $O_{33} = -0.31$, $O_{11} - O_{22} = +0.09$ (4-cyano-4'-pentylbiphenyl, 294 K).

Since the hyperfine shifts of nonproton nuclei (^{13}C, ^{19}F, $^{35}Cl/^{37}Cl$) are essentially determined by the π spin populations at these centers, it is fairly straightforward to calculate the π spin populations from the tensor components A'_{33}:

$$A'_{33} = B_{33}\rho_\pi \quad (6)$$

where the factor B_{33} depends on the particular nucleus. The following values of B_{33} were obtained from SCF calculations: 181.6 MHz (^{13}C), 3030 MHz (^{19}F), and 280.6 MHz (^{35}Cl).[31] The outlined procedure yields the following experimental estimates for the spin populations in phenalenyl from the ^{13}C shifts: $\rho_1 = 0.202$ and $\rho_2 = -0.057$. These values are close to those obtained from SCF calculations ($\rho_1 = 0.219$, $\rho_2 = -0.064$).[32] Furthermore, the spin populations at the halogen atoms can be estimated as $\rho_F = -0.009$ (**2a**) and $|\rho_{Cl}| \simeq 0.006$ (**3a**). Finally it should be pointed out that the experimental data on the isotropic ^1H coupling

(30) H. R. Falle and G. R. Luckhurst, *J. Magn. Reson.*, **3**, 161 (1970).
(31) N. M. Atherton, "Electron Spin Resonance", Ellis Horwood, Chichester, 1973, p 131.
(32) L. C. Snyder and T. Amos, *J. Chem. Phys.*, **42**, 3670 (1965).

constants and the isotropic and anisotropic ^{13}C couplings (see Tables I and III) demonstrate that chloro or fluoro substitution in position 2 alters the spin populations by 1% at most. An exception might be position 2, since the respective ^{13}C shift in **3c** is increased by about 15%. The strong change in the *isotropic* ^{13}C coupling, however, is certainly mainly due to different spin polarization properties of the C–Cl bond as compared to the C–H bond.[29]

Relaxation Behavior. It is usually found that the relaxation behavior of ^{13}C ENDOR lines is quite different from that of ^{1}H ENDOR lines provided the spin population at the ^{13}C atom and therefore the hyperfine anisotropy is large.[12,13] Thus, higher temperatures and rf field amplitudes are required for a maximum ^{13}C ENDOR response; strong cross-relaxation effects are observed and the lines are broadened. This can be understood by considering the influence of the electron–nuclear dipolar interaction, i.e., the hyperfine anisotropies $\mathrm{Tr}(A'^2)$, on the relaxation rates and line widths. The relaxation rates are given by the following equations if only the electron–nuclear dipolar contributions have to be considered ($S = {}^1/_2$, $I = {}^1/_2$):[33]

$$W_n = (\pi^2/10)\mathrm{Tr}(A'^2)\tau_C \tag{7}$$

$$W_{x1} = (\pi^2/15)\mathrm{Tr}(A'^2)\tau_C/(1 + \omega_e^2\tau_C^2) \tag{8}$$

$$W_{x2} = 6W_{x1} \tag{9}$$

where τ_C is the rotational correlation time, W_n is the nuclear spin relaxation rate, and W_{x1} and W_{x2} are the cross-relaxation rates involving simultaneous electron–nuclear spin flips (flip–flop and flop–flop). The electron spin–lattice relaxation rate, W_e, is usually governed by the spin–rotational interaction, $W_e \propto \tau_C^{-1}$.

From calculated anisotropic hyperfine components,[7,29,34] the magnitudes of $\mathrm{Tr}(A'^2)$ for the different kinds of nuclei present in ^{13}C-labeled phenalenyl can be estimated as follows: $\mathrm{Tr}(A'^2)$ = 2300 MHz^2 (1-^{13}C), 250 MHz^2 (2-^{13}C), 150 MHz^2 (1-^{1}H), and 10 MHz^2 (2-^{1}H). This shows that the nuclear spin relaxation rate (eq 7) of ^{13}C in position 1 should be larger than that of the protons by a factor of 15 or 230, respectively. From the results of the liquid-crystal measurements it can be concluded that the hyperfine anisotropy of ^{19}F in **2a** is not much less than that of 1-^{13}C in **1b**, $\mathrm{Tr}(A'^2) \simeq 1100$ MHz^2; therefore the relaxation behavior should be similar.

The ENDOR line width of a nucleus i is given approximately by[27b,35]

$$T_{2n}^{-1} = (2\pi^2/15)\mathrm{Tr}(A_i'^2)\tau_C + (\pi^2/10)\sum_{j\neq i}\mathrm{Tr}(A_j'^2)\tau_C + W_e \tag{10}$$

Provided the rotational correlation time τ_C is short (vide infra), the electron–nuclear dipolar contribution to the line widths will be negligible. Then the line widths should be determined by the electron spin relaxation rate W_e and therefore be equal for the different kinds of nuclei. This is just what is observed for the ^{13}C-labeled phenalenyls in toluene at elevated temperatures; i.e., the line widths are fairly small (about 60 kHz) under these conditions, provided the concentration is kept low to avoid Heisenberg exchange effects, since the spin–rotational contribution to W_e being proportional to $(g_{ii} - g_e)^2$ (the deviations of the **g** tensor components from the free electron value $g_e = 2.002\,319$) is not very large in the case of the hydrocarbon radical phenalenyl ($g_{xx} = g_{yy} = 2.002\,78$, $g_{zz} = 2.002\,26$).[7,10b]

To achieve a maximum ENDOR enhancement, it is necessary to fulfill the saturation condition for the nuclear spin transitions $\sigma_n = (1/4)\gamma_n^2 B_n^2 \Omega_n T_{2n} \geq 1$, where Ω_n is Freed's nuclear spin–lattice relaxation parameter[36] ($\Omega_n \simeq 2/W_n$) and B_n the effective rf field at the nucleus, $B_n = \kappa B_n'$ (B_n' is the external rf field and $\kappa = \nu_{ENDOR}/\nu_n$, the hyperfine enhancement factor[37]). In fact, although

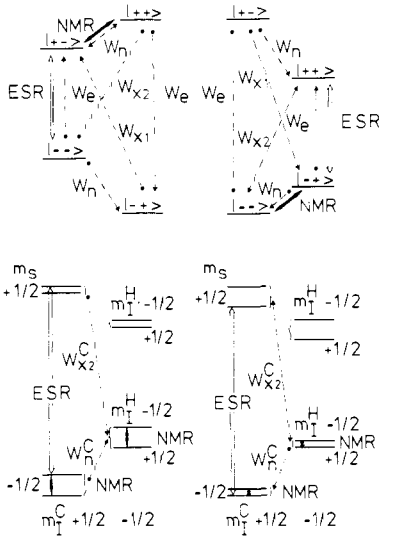

Figure 9. Top, energy-level diagrams for the coupling of an electron ($S = {}^1/_2$) with one nucleus ($I = {}^1/_2$, $|a/2| > \nu_n$; left, $a > 0$; right, $a < 0$). Bottom, energy-level diagrams for the coupling of an electron with a ^{13}C nucleus ($a_c > 0$) and a proton (left, $a_H > 0$; right, $a_H < 0$) (see text).

saturation of the (low-frequency) ^{13}C ENDOR line belonging to position 1 could not quite be achieved with applied rf fields up to 0.85 mT (in the rotating frame), fairly strong signals were obtained at elevated temperatures. This can be understood since the high value of $\mathrm{Tr}(A'^2)$ giving rise to large nuclear spin lattice relaxation rates, W_n, can be compensated for by selecting the experimental conditions such that the rotational correlation time, τ_C, becomes small ($\tau_C \propto \eta/T$) (see eq 7).

Whereas the magnitude of W_n decreases with decreasing τ_C (i.e., decreasing η/T), the cross-relaxation rates W_{x1} and W_{x2} show a different τ_C dependence (see eq 8 and 9). Therefore these cross-relaxation rates become the dominant relaxation rates at elevated temperatures. This is evident from the dependence of the intensity pattern of the ENDOR spectra on the ESR component being saturated, vide infra.

Finally some remarks concerning the rotational correlation time, τ_C, shall be added. It is usually possible to estimate τ_C from the Stokes–Einstein relation[36]

$$\tau_C = 4\pi r^3\eta/3kT \tag{11}$$

where r is an effective rotational radius of the tumbling molecule in solution, η the viscosity of the solvent, and T the temperature of the medium. However, considering the axially symmetric, disklike shape of the phenalenyl radical, the rotational motion of this radical cannot be adequately described by a single correlation time. In fact, the rotational motion of *unsubstituted* phenalenyl about its symmetry axis is always rapid with respect to the ESR/ENDOR time scale, in fluid solution and even in solid matrices.[10b] As a consequence, the hyperfine anisotropy of the large proton splitting which is only large *in the molecular plane* (i.e., $|A'_{11}|, |A'_{22}| \gg |A'_{33}|$) is effectively averaged out. This is evident from the ESR and ENDOR line widths of **1a** in highly viscous solvents and from the temperature dependence of the ENDOR response. On the other hand, the ^{13}C hyperfine tensors are essentially axially symmetric, the largest anisotropic component being the out-of-plane component A'_{33}. Since the correlation time for a rotational motion about an in-plane axis is comparatively large in highly viscous solvents (e.g., mineral oil at room temperature), a substantial line broadening is found for phenalenyl-*1*-^{13}C and the relaxation rate W_n^C becomes very large. Yet this correlation time is strongly temperature dependent (eq 11); therefore the influence of the ^{13}C hyperfine anisotropy on the ESR and ENDOR line widths becomes vanishingly small for solvents of low viscosity at elevated temperatures (e.g., toluene at room

(33) Reference 31, p 383.
(34) H. R. Falle and M. A. Whitehead, *Can. J. Chem.*, **50**, 139 (1972).
(35) J. H. Freed and G. K. Fraenkel, *J. Chem. Phys.*, **39**, 326 (1963).
(36) J. H. Freed, "Multiple Electron Resonance Spectroscopy", M. M. Dorlo and J. H. Freed, Eds., Plenum Press, New York, 1979, p 73.
(37) S. Geschwind, "Hyperfine Interactions", A. J. Freeman and R. B. Frankel, Eds., Academic Press, New York, 1967.

temperature) (see Figures 2 and 4).

Cross-Relaxation Effects. The most salient feature of the ENDOR spectra taken from the radicals containing ^{13}C and ^{19}F nuclei is certainly the strong dependence of the intensity pattern on the field setting (see Table II). First the nonproton ENDOR lines shall be considered. It is always found that the high- (low-) frequency ENDOR line is more (less) intense when a low-field ESR component (i.e., $aM_I > 0$) is saturated as compared to the high-field setting ($aM_I < 0$). The various possible spin–lattice relaxation processes are given in Figure 9 (top). For instance, if a high-field ESR component is saturated and the low-frequency NMR transition is irradiated, a relaxation pathway is provided via a W_{x2} process *irrespective of the sign of the hyperfine coupling.* On the other hand, if the high-frequency NMR transition is irradiated, relaxation may proceed via a W_{x1} process. It is evident from eq 9 that the W_{x2} process is much more efficient than the W_{x1} process if the electron-nuclear dipolar mechanism governs these relaxation rates. Actually this is found experimentally, although the amplitude ratio R (see Table II) does not reach the theoretical limit of 9.[38]

Moreover, not only the ^{13}C or ^{19}F ENDOR amplitudes but also the ^1H ENDOR amplitudes are affected by cross-relaxation effects. These effects are not caused by the protons themselves for the following reasons. Firstly, the saturated ESR components were associated with nuclear spin configurations having total magnetic quantum numbers $M_I^H = 0$ for both sets of equivalent protons (except for the small proton coupling in **1b,c**). Secondly, it was checked independently by saturating different ESR components in **1a** that the intensity pattern did not change. Consequently, the strong cross-relaxation effects of the nonproton nuclei must also affect the relaxation behavior of the protons. A similar effect has been found recently in the study of pyrazine radical anions.[16] It is obvious from Figure 9 (bottom) that a W_{x2} process associated with a nonproton nucleus can only provide a relaxation pathway for either the high or the low frequency ^1H NMR transition depending on the relative signs of the couplings and on the ESR component being saturated. For instance, if the low-field ESR transition ($a^C M_I^C > 0$) is saturated, the intensity of the high-frequency ^{13}C ENDOR line would be enhanced. Considering the protons, the intensity of the high-frequency ^1H ENDOR line is enhanced if sign (a^H) = sign (a^C) whereas the intensity of the low-frequency ^1H ENDOR line is enhanced if sign (a^H) $\neq$ sign (a^C). Thus, the intensities are affected in the same way as in a general TRIPLE experiment allowing the determination of the relative signs,[15] which can be illustrated by inspection of Tables I and II. For example, in **1b** $R > 1$ for a_1^C and a_2^H, $R < 1$ for a_1^H, whereas in **1c** $R > 1$ for a_2^C and a_1^H, $R < 1$ for a_2^H. This is consistent with the assignment of positive signs to a_1^C and a_2^H and negative signs to a_2^C and a_1^H. The situation becomes much more complicated if a radical contains two different nuclei exhibiting strong cross-relaxation effects, e.g., ^{13}C and ^{19}F in **2b**. In that case, the effect of each nucleus separately as well as the mutual interaction have to be considered. Actually, opposite signs can be deduced for a^F and a_1^C from the results obtained for **2b**.

Rearrangement Reaction. The spectral evidence provided by NMR, ESR, ENDOR, and ENDOR-induced ESR demonstrates that in the reaction **7b** → **8b** (**7d** → **8d**) a rearrangement must occur. Thus, instead of pure **8b** a mixture of 84.5% **8b** and 15.5% **8c** is obtained, and instead of pure **8d** a mixture of 69% **8d** and 31% **8e**. Although the result obtained with the deuterium label might be explained by assuming an intramolecular proton shift, the ^{13}C results clearly prove that the carbon skeleton rearranges. Moreover, the numerical results of the two sets of experiments, which seem to disagree at first sight, can be accounted for by a consistent mechanism. It seems reasonable to assume that during the reaction some kind of carbonium ion is formed by elimination of nitrogen from the diazonium ion prepared from **7b** (**7d**). The position of the substituent in **7a** as well as in **8a** is known to be *exo*.[39] In order to account for the retention of configuration in the reaction, Pettit suggested an S_Ni mechanism.[18] This possibility can now be ruled out in view of our results. The observed rearrangement requires the intermediate breaking of the carbon–carbon bond between C-atoms 6a and 6b or 7a and 7b. We think that the reaction is best described by a Wagner–Meerwein-type rearrangement. Since an aromatic group migrates from position 6b or 7a to 7, it is likely that a phenonium ion will be the intermediate.[40] With the assumption that this intermediate is symmetric, the following distribution of products is expected for the rearrangement reaction. Starting with the diazonium ion from **7b**, there is a 50% chance of breaking either bond 6a–6b or 7a–7b. If the latter course is taken, the position of the ^{13}C label will remain unaltered. Otherwise there is an equal chance that the intermediate will yield either **8b** or **8c**; i.e., the product distribution will be 75% **8b** and 25% **8c**. Starting with **7d** (or **7c**), it does not matter which C–C bond is broken in the formation of the intermediate. Depending on which bond is broken in the intermediate to yield the product, either **8d** or **8e** is formed, in a ratio of 50:50. Our data are not quite in agreement with this picture. We conclude that either the rearrangement mechanism accounts for only part of the products (62% rearrangement, 38% "direct" substitution) or that the intermediate is not symmetric. Further investigations and calculations are in progress.

Conclusion

It has been demonstrated that ^{13}C ENDOR signals of ^{13}C labeled phenalenyls can easily be observed provided the rotational correlation time is kept short (low viscosity of the solvent and elevated temperatures, e.g., toluene at room temperature). Under these conditions, the ^{13}C ENDOR lines are fairly narrow (width $\simeq$ 60 kHz) in spite of the large hyperfine anisotropy. A remarkable feature of the ENDOR spectra is the fact that the intensity pattern not only of the ^{13}C lines but also of the ^1H lines is strongly influenced by cross-relaxation effects. Since this effect is analogous to the intensity change caused by irradiation of a second NMR transition in a general TRIPLE experiment, it can serve equally well for the relative sign determination of hyperfine coupling constants. The method requires the presence of a nucleus exhibiting large hyperfine anisotropy (e.g., ^{13}C, ^{14}N, ^{19}F) and short rotational correlation times. The rearrangement reaction taking place in one of the synthetic pathways to phenalenyl can tentatively be described as a Wagner–Meerwein-type rearrangement which is not observable in the case of unlabeled, unsubstituted compounds.

Experimental Section

Instrumentation. Infrared spectra (in KBr) were recorded on a Perkin-Elmer PE 580 B spectrometer (double beam, double monochromator) connected to a data station (Perkin-Elmer CDS-3500). The mass spectra were recorded on a 112S or CH5-DF Varian MAT spectrometer with low voltages (11 to 20 eV) for the determination of the isotopic contents. The ^1H and ^{13}C NMR spectra were taken on a Bruker WH-270 (frequency 270 or 67.89 MHz, respectively) with a 10-mm diameter sample tube and $CDCl_3$ or trifluoroacetic acid-*d* solvent ($\delta_{^{13}CDCl_3}$ 77 and $\delta_{^{13}CF_3COOD}$ 130 with respect to tetramethylsilane). ESR spectra were recorded on an AEG 20XT or a Bruker ER 200D ESR spectrometer. The ENDOR and TRIPLE instrumentation basically consists of a Bruker ER 220D ESR spectrometer equipped with a Bruker cavity (ER200ENB) and home-built NMR facilities described elsewhere.[41] ENDOR spectra were accumulated by using a Nicolet signal averager 1170 employing 1K data points; typically 64 or 128 sweeps were taken, 30 s per scan. Microwave power levels of 2, 4, and 12 mW were applied in the case of **1b**, **2b**, and **3b**, respectively, and an rf power of about 20–50 W corresponding to a field strength of 0.3–0.5 mT in the rotating frame (not constant over the frequency range).

Preparation of Compounds. The ^{13}C-labeled compounds were prepared from $Ba^{13}CO_3$ as ^{13}C source with an approximate isotopic enrichment of (a) 90% or (b) 98% (Monsanto). Due to the high price of $Ba^{13}CO_3$ all synthetic steps involving $^{13}CO_2$ were performed in an apparatus, allowing the $^{13}CO_2$ to escape from the parent $Ba^{13}CO_3$ and subsequent organometallic reaction under vacuum conditions.[42]

(38) H. van Willigen, M. Plato, R. Biehl, K. P. Dinse, and K. Möbius, *Mol. Phys.*, **26**, 793 (1973).

(39) V. Rautenstrauch and F. Wingler, *Tetrahedron Lett.*, 4703 (1965).
(40) D. J. Cram, *J. Am. Chem. Soc.*, **71**, 3863 (1949).
(41) H.-J. Fey, H. Kurreck, and W. Lubitz, *Tetrahedron*, **35**, 905 (1979).

(1-Naphthyl)acetic-*carboxyl*-^{13}C Acid (9b). The Grignard reagent from 15 g (85 mmol) of (1-chloromethyl)naphthalene and 2.1 g of Mg in 75 mL of ether was allowed to react with $^{13}CO_2$ from 10 g (50 mmol) of $Ba^{13}CO_3$ at −50 to −40 °C (2–3 h). Hydrolysis (100 mL of 2 N HCl added dropwise), ether extraction, and repeated purification via the Na salt yielded 7.1–8.4 g of **9b** (76–90%), mp 129–30 °C, ^{13}C contents (MS) (a) 90.9%, (b) 99.0%.

(1-Naphthyl)acetyl-*carbonyl*-^{13}C Chloride (10b). A 14-g (75 mmol) sample of **9b** and 50 mL of thionyl chloride were stirred for 2 h at 60–65 °C. After evaporation of the solvent the residue was distilled in a bulb tube: yellow or red oil, yield 15.1 g (98%), bp 130–135 °C (0.15 mbar), ^{13}C contents (MS) (a) 91.2%, (b) 99.4%.

1-Acenaphthen-*1*-^{13}C-one (11b). To 13.1 g (64 mmol) of **10b** in 85 mL of CH_2Cl_2 14 g of $AlCl_3$ were added in portions. (Alternatively, **10b** may be dropped into a suspension of $AlCl_3$). A slightly exothermic reaction with frothing results. After it was stirred for 3 h, the dark green solution was poured into ice water. The product was isolated by extraction (CH_2Cl_2) and usual workup, yielding a solid or a dark oil. Purification by column chromatography (silica gel/CH_2Cl_2) and sublimation (110 °C, 0.15 mbar) gave a white solid: yield 5.14 g (48%), mp 120–121 °C, ^{13}C contents (MS) (a) 91.5%, (b) 99.5%.

1-Acenaphthen-*1*-^{13}C-ol (12b). To 4.45 g (26 mmol) of **11b** in 80 mL of THF 1.5 g of $LiAlH_4$ was added in small portions with stirring and ice cooling. After stirring at room temperature for several hours and 6 h of reflux the mixture was hydrolyzed (150 mL of 1 N HCl added dropwise, ice cooling), concentrated to about one-half its volume, and extracted with CH_2Cl_2 (three portions of 150 mL). Usual workup gave a yellow solid which was purified by recrystallization (benzene) and sublimation (135 °C, 0.15 mbar): white solid, yield 3.00 g (68%), mp 144.5–145 °C, ^{13}C contents (MS) (a) 92.7%, (b) 99.0%.

1-Acenaphthylene-*1*-^{13}C (13b). A 2.0-g (12 mmol) sample of **12b** was refluxed in 130 mL of glacial acetic acid for 30 h. After evaporation of the solvent, the residue was purified by column chromatography (150 g of neutral Al_2O_3, activity grade I/pentane): yellow platelets, yield 1.08 g (60%), mp 90.5–91.5 °C, ^{13}C contents (MS) (a) 92.1%, (b) 99.0%.

6b,7a-Dihydro-7*H*-cycloprop[*a*]acenaphthylene-*6b*-^{13}C-7-carboxylic acid (5b) was prepared by refluxing 8.3 g (54 mmol) of **13b** in toluene with 12 g of ethyl diazoacetate according to ref 20. The ester **4b** was hydrolyzed with NaOH (10%) and the resulting Na salt treated with norite. The solution was acidified with concentrated HCl, the precipitate was collected and dried over P_2O_5: yield 2.32 g (20%), mp 193–195 °C, ^{13}C contents (MS) (a) 90.0%.

6b,7a-Dihydro-7*H*-cycloprop[*a*]acenaphthylene-*6b*-^{13}C-7-carboxylic acid chloride (6b) was prepared by refluxing 2.1 g (9.9 mmol) of **5b** in 11 mL of benzene with 8 mL of thionyl chloride according to ref 20. The solvent was evaporated and the remaining oil treated with pentane. Evaporation gave a dark brown solid: yield 2.24 g (98%), mp 68–72 °C, ^{13}C contents (MS) (a) 91.9%.

7-Amino-6b,7a-dihydro-7*H*-cycloprop[*a*]acenaphthylene-*6b*-^{13}C hydrochloride (7b) was prepared according to ref 18; 2.2 g (9.6 mmol) of **6b** in 11 mL of acetone (−7 °C) and 0.9 g of NaN_3 (in 4.5 mL of H_2O) gave the azide which was separated and refluxed in benzene for 5 h. After evaporation of the solvent, the residue was refluxed for 1 h in concentrated HCl (10 mL + 3 mL). The brown precipitate obtained on cooling was collected: yield 1.7 g (81%), ^{13}C contents (MS) (a) 91.7%.

7-Chloro-6b,7a-dihydro-7*H*-cycloprop[*a*]acenaphthylene-*6b*-^{13}C (8b) was prepared according to ref 18. To a suspension of 1.65 g (7.5 mmol) of **7b** in a mixture of 14 mL of concentrated HCl, 7 mL of acetic acid, and 35 mL of ether a solution of 0.75 g of $NaNO_2$ in 3.5 mL of H_2O was added with stirring at −7 °C. After 15 min in the freezing mixture and 30 min at room temperature, water was added and the product extracted with ether (six portions of 40 mL). The combined organic phases were washed (water, 5% aqueous NH_3), dried (Na_2SO_4), and evaporated. The brown crude product was suspended in benzene/pentane (1:3) and purified by column chromatography (70 g of neutral Al_2O_3, activity grade I; pentane/benzene 10:1). Evaporation of the solvent gave white needles: yield 0.66 g (43%), mp 117–119 °C, ^{13}C contents (MS) (a) 90.7%. The obtained **"8b"** is actually a mixture of the isotopic isomers **8b** and **8c** (see text).

6b,7a-Dihydro-7*H*-cycloprop[*a*]acenaphthylene-*1,2,3,4,5,6,6b,7a*-d_8-7-carboxylic acid chloride (6d) was prepared in analogy to **6b** from 2.05 g (9.4 mmol) of **5d**:[6] yield 2.22 g (99%), mp 68–71 °C, isotopic composition (MS) 96.5% D_8, 3.5% D_7.

7-Amino-6b,7a-dihydro-7*H*-cycloprop[*a*]acenaphthylene-*1,2,3,4,5,6,6b,7a,N,N*-d_{10} hydrochloride-*d* (7d) was prepared in analogy to **7b** from 2.15 g (9.1 mmol) of **6d** with the following modification. The isocyanate was refluxed in DCl (35%, 11 mL + 4 mL) instead of HCl. Yield was 1.6 g (77%).

7-Chloro-6b,7a-dihydro-7*H*-cycloprop[*a*]acenaphthylene-*1,2,3,4,5,6,6b,7a*-d_8 (8d) was prepared in analogy to **8b** from 1.45 g (6.3 mmol) of **7d**: yield 0.56 g (42%), mp 118–119 °C, isotopic composition (MS) 97.1% D_8, 2.9% D_7. The obtained **"8d"** is actually a mixture of the isotopic isomers **8d** and **8e** (see text).

3-(1-Naphthyl)propanoic-*carboxyl*-^{13}C Acid (14b). The Grignard reagent from 14.1 g (60 mmol) of 1-(2-bromoethyl)naphthalene[19] and 1.5 g of Mg in 50 mL of ether was allowed to react with $^{13}CO_2$ from 10 g (50 mmol) of $Ba^{13}CO_3$ (−50 to −40 °C). Hydrolysis, extraction with ether, and purification via the Na salt yielded 7.84 g of **14b** (78%), mp 155 °C (from benzene), ^{13}C contents (MS) (b) 98.5%.

1-Phenalen-*1*-^{13}C-one (15b) was prepared according to ref 43 from 2.47 g (12.3 mmol) of **14b** and 13 mL of $SnCl_4$ (120 °C, 3 h). After cooling, the clear solution (containing unreacted **14b**) was decanted and the black residue boiled in acetone with norite. After removal of the solvent, the product was taken up in benzene, washed with water, and purified by column chromatography (silica gel/$CHCl_3$): yield 0.2 g (44%).

Phenalene-*1*-^{13}C (16b) was prepared according to ref 44; 1.05 g of $AlCl_3$ and 0.14 g of $LiAlH_4$ in 50 mL of ether were refluxed with 0.2 g (1.1 mmol) of **15b** (in benzene; 1.5 hr). Hydrolysis (dilute HCl), extraction with ether, and purification by column chromatography (silica gel/$CHCl_3$) yielded 0.14 g of **16b** (78%).

Generation of Radicals. The phenalenyl radicals were generated by one of the following four methods. (A) Solutions of phenalenes (**16a,b**) were heated in the presence of atmospheric O_2 for a few minutes. (B) Solutions of the precursors **8a,b,d** were heated in the ESR sample cell. (C) Solutions of the carboxylic acids **5a,b,d** were converted to suspensions of the mercury salts by mixing with HgO and then heated strongly.[6] (D) 2-Chlorophenalenyls (**3a,b,c,bc**) formed in an exothermic reaction on mixing acenaphthylene (**13a** or **13b**) with potassium *tert*-butanolate and a few drops of $CHCl_3$ ($^{13}CHCl_3$). Generation of 2-fluorophenalenyls (**2a,b**) required strong heating (Bunsen burner) of sodium trifluoroacetate with solutions of acenaphthylene (**13a** or **13b**). Solvents used were toluene, mineral oil (Shell Ondina G17 or G33), Nematic Phase IV Licristal (Merck), and 4-cyano-4′-pentylbiphenyl. All solutions were carefully deoxygenated prior to ESR/ENDOR measurements by flushing with purified N_2.

Acknowledgment. We thank E. Brinkhaus for collaboration. We also thank U. Ostwald (MS), J. Erdmann (IR) and M. Brauer and Dr. K. Roth (NMR). H.K. gratefully acknowledges financial support by Deutsche Forschungsgemeinschaft (Normalverfahren) and Fonds der Chemischen Industrie. B.K. gratefully acknowledges a Liebig stipend of the Fonds der Chemischen Industrie.

Registry No. 1a, 16481-29-1; **1b**, 87682-86-8; **1c**, 87682-90-4; **1d**, 87682-91-5; **2b**, 87682-87-9; **3b**, 87682-88-0; **3bc**, 87682-89-1; **5b**, 87682-97-1; **6b**, 87682-98-2; **6d**, 87683-01-0; **7b**, 87682-99-3; **7d**, 87683-02-1; **8b**, 87683-00-9; **8c**, 87683-07-6; **8d**, 87683-03-2; **8e**, 87683-08-7; **9b**, 87682-92-6; **10b**, 87682-93-7; **11b**, 87682-94-8; **12b**, 87682-95-9; **13b**, 87682-96-0; **14b**, 87683-04-3; **15b**, 87683-05-4; **16b**, 87683-06-5.

(42) W. G. Dauben, J. C. Reid, and P. E. Yankwich, *Anal. Chem.*, **19**, 828 (1947). H. R. Schütte, "Radioaktive Isotope in der Organischen Chemie und Biochemie", Verlag Chemie, Weinheim, 1966.

(43) J. W. Cock and C. L. Hewett, *J. Chem. Soc.*, 365 (1934).

(44) R. M. Pagni and C. R. Watson, *Tetrahedron*, **29**, 3807 (1973).